frontiers | Frontiers in Environmental Science

TYPE Original Research
PUBLISHED 23 October 2023
DOI 10.3389/fenvs.2023.1281341

OPEN ACCESS

EDITED BY
Mezbaul Bahar,
The University of Newcastle, Australia

REVIEWED BY
Ying-heng Fei,
Guangzhou University, China
Qingqing Huang,
Chinese Academy of Agricultural Sciences, China

*CORRESPONDENCE
Mengying Si,
simysmile@csu.edu.cn

RECEIVED 22 August 2023
ACCEPTED 12 October 2023
PUBLISHED 23 October 2023

CITATION
Yang Z, Zeng G, Liu L, He F, Arinzechi C, Liao Q, Yang W and Si M (2023), Simultaneous immobilization of lead, cadmium and arsenic in soil by iron-manganese modified biochar. *Front. Environ. Sci.* 11:1281341. doi: 10.3389/fenvs.2023.1281341

Simultaneous immobilization of lead, cadmium and arsenic in soil by iron-manganese modified biochar

Zhihui Yang[1,2], Gai Zeng[1], Lin Liu[1], Fangshu He[1], Chukwuma Arinzechi[1], Qi Liao[1,2], Weichun Yang[1,2] and Mengying Si[1,2]*

[1]Department of Environmental Engineering, School of Metallurgy and Environment, Central South University, Changsha, China, [2]Chinese National Engineering Research Center for Control and Treatment of Heavy Metal Pollution, Changsha, China

Cationic lead/cadmium and anionic arsenic exhibit opposite geochemical behaviors in soils, which makes the synchronous remediation of As, Cd, and Pb challenging. In this study, we developed an iron-manganese modified biochar (BC-Fe-Mn) that prepared from straw with iron (Fe) and manganese (Mn) loading at a pyrolysis temperature of 550 °C. After BC-Fe-Mn immobilization for 90 days, the simultaneous immobilization efficiency of Pb, Cd, and As reached 57%, 51%, and 35%, respectively. Speciation distributions shows that As transformed from specific bound state into weakly low crystallinity iron bound state. Cd transformed from carbonate fraction into Fe-Mn oxide bound fraction, and Pb transformed from carbonate fraction into residual state. During the procedure, simultaneous immobilization mechanisms might involve heavy metal morphological transformation, precipitation/co-precipitation, and surface complexation. Cd and Pb absorbed onto BC-Fe-Mn. Then the increased free iron oxides (Fe_d) reacted with the dissolved As to form iron-arsenic precipitation. The results show that BC-Fe-Mn is a promising material for the simultaneous immobilization of Pb, Cd, and As in multi-metal contaminated soil.

KEYWORDS

biochar, lead, cadmium, arsenic, immobilization

Highlights

- BC-Fe-Mn has been prepared to immobilize Pb, Cd, and As.
- Simultaneous immobilization efficiency of Pb, Cd, and As reached 57%, 51%, and 35%, respectively.
- Cd and Pb absorbed onto BC-Fe-Mn and the increased free iron oxides reacted with the As to form Fe-As precipitation.

1 Introduction

As a vital resource for human survival, soil plays a crucial role in the process of human progress and development. Due to human activities such as non-ferrous metal mining and industrial waste disposal, the content of heavy metals continuously accumulates in soil and

exceed the safety threshold. As reported, more than 13,300 ha in China are polluted by cadmium, with 18.6% considered moderately or lightly polluted, and 7.1% heavily polluted (GAO et al., 2016). According to the 2014 Soil Pollution Survey Report of China, lead (Pb), cadmium (Cd), and arsenic (As) pollution made up 70% of the excess ratio of heavy metal pollution in China. It pose a serious threat to human health through the bioaccumulation and food chain (TóTH et al., 2016). Therefore, an effective technique for simultaneous reducing the toxicity of the Pb, Cd and As in soil was urgently necessary.

Immobilization is advocated due to its easy-operate and high-efficiency properties (IGALAVITHANA et al., 2019). However, the pollution control of Pb, Cd, and As in soil is mainly concentrated on single heavy metals or two at most. There are few studies on the simultaneous stabilization of Pb, Cd, and As. In fact, cationic lead/cadmium and anionic arsenic exhibit opposite chemical behaviors in soil. For example, an increase in soil pH can increase the desorption of As on the soil surface due to the increasing the electronegativity of arsenate and soil particles. Pb and Cd are usually positively charged. When the pH is raised, Pb and Cd can be effectively immobilized (YANG X. et al., 2018). Therefore, their opposite chemical behavior poses a significant challenge for simultaneous immobilization of Pb, Cd, and As in soil.

Biochar (BC) is widely used in remediation of heavy metal contaminated soil (LYU et al., 2018). As compared with other materials, BC is a readily stable carbon-rich material with available porous, high specific surface area. It can increase the cation exchange capacity (CEC) and reduce the availability of heavy metals in soil through precipitation and surface immobilization (LI et al., 2019; TU et al., 2020; LV et al., 2021). Furthermore, an appreciable amount of oxygen-containing groups are contained on the surface, which show high efficiency adsorption of heavy metal cations (CHEN et al., 2021). However, due to the negatively charged surfaces of BC, its ability to remove arsenic anion pollution is clearly limited. For example, Yang's study showed that BC has high stabilization efficiency for Pb, but the immobilization efficiency of arsenic is low (YANG X. et al., 2018). Therefore, it is necessary to modify BC for simultaneous immobilization of Pb, Cd, and As in soil.

Iron/manganese material is characterized by its high reactivity, specific surface area, and surface charge. Fe/Mn-based materials possess strong affinity for As through the formation of surface complexes or precipitates and have been widely used for As immobilization. It can promote the changes of the self-generated structure and surface properties of iron oxides to increase the adsorption capacity of heavy metals in soil (TACK et al., 2006). However, simple iron-manganese compounds exhibit limited adaptability to the soil environment and may even catalyze the activation of other heavy metals in the soil. The products of biochar combined with iron (or manganese) can overcome their shortcomings and give full play to the advantages of BC and iron (or manganese).

Recent reports showed that fabrication the Fe/Mn onto biochars seems a promising strategy to improve the efficiency of simultaneous immobilization of As with Cd and Pb. It has been reported biochar with zero-valent iron (BC-ZVI) has a good removal effect on As by reducing As(V) to As(III) and conformal substitution of As(III) and Fe(III) in the newly formed FeOOH (BAKSHI et al., 2018). The hydroxyl groups on iron oxides can effectively adsorb As and form precipitates (FU et al., 2017). As can also undergo coordination reactions on the surface of manganese oxides to form As-MnO_2 complexes (VILLALOBOS et al., 2014). After modified with the iron and/or manganese, the number of functional groups on the surface of BC, such as carboxyl, hydroxyl, and phenolic hydroxyl, can be significantly increased, which can form oxygen-containing complexes with heavy metal ions via stabilization absorption configurations (O'REILLY and HOCHELLA, 2003; SONG et al., 2014; LI et al., 2017). Moreover, studies have shown that iron-manganese composites have an excellent ability to remove lead from solution due to the interaction between active functional carboxyl groups and hydroxyl groups on the surface (REN et al., 2012; HU et al., 2017). Manganese-iron binary oxide-biochar composite (FMBC) with good adsorption of Cd and copper (Cu) was prepared via impregnation/sintering method (ZHOU et al., 2018). Therefore, the combination of BC and iron-manganese materials possess great potential to overcome their respective shortcomings for the simultaneous immobilization of Pb, Cd, and As in soil.

This research hopes to develop an iron-manganese modified BC material to simultaneous immobilized the Pb, Cd, and As in multi-metal contaminated soil. The transformation process of Pb, Cd, and As in soil were studied by analyzing the speciation distribution of heavy metals and the properties of iron-manganese particles in soil. This study will provide a reliable strategy for the remediation of multi-metal contaminated soil.

2 Materials and methods

2.1 Soil pretreatment and characterization

Contaminated soil samples were collected from an abandoned factory in Changde, China. The samples were air-dried and crushed at room temperature, and thoroughly mixed after removing stones and plant rhizomes. The mixed soil was passed through a 20–100 mesh screen, and then digested using a mixture of HNO_3-HCl-HF to determine the total concentration of Pb, Cd, and As using K. Kameda's method (KAMEDA et al., 2017). The extraction of soil free iron oxide (Fe_d) was conducted using the dithionite-citric acid-bicarbonate procedure, whereas the extraction of soil amorphous iron oxide (Fe_o) was carried out using a solution of 0.2 mol L^{-1} ammonium oxalate. The concentration of crystalline iron oxide (Fe_c) was determined by subtracting the Fe_o content from the total Fe_d content. (CUI et al., 2020). All digested and extracted samples were measured by inductively coupled plasma optical emission spectrometry (ICP-OES, TCP-5100-VDV). The As in soil were extracted by sodium bicarbonate and measured by atomic fluorescence spectrometer (HGF-V2). Cation exchange capacity (CEC) was determined using the 1 mol L^{-1} NH_4Ac method (SONG et al., 2017). The properties of soil samples are exhibited in Table 1.

2.2 Preparation of modified BC and characterization

The preparation of BC and modified BC are as follows: the rice straw (obtained from Changsha city, China) was soaked in an

TABLE 1 Heavy metal content in soil.

Properties	Value
Soil pH	6.55
CEC (cmol/kg)	5.28
Total Pb (mg kg^{-1})	1800
Total Cd (mg kg^{-1})	69
Total As (mg kg^{-1})	650
DTPA-extractable Pb (mg kg^{-1})	1,200
DTPA-extractable Cd (mg kg^{-1})	61
$NaHCO_3$-extractable As (mg kg^{-1})	80

appropriate amount of deionized water and stirred for 2 h followed by drying in a constant temperature oven at 105 °C for 24 h and ground into powder. The powder was then sifted via a 40-mesh griddle. 10 g of rice straw powder was then pyrolyzed at a rate of 5 °C·min^{-1}–550 °C for 2 h in a controlled atmosphere furnace under N_2 atmosphere. As-prepared solid was washed quickly with ethanol and deionized water for 3–4 times, and finally dried in a drying oven under N_2 atmosphere to obtain BC.

10 g of rice straw powder was soaked in 175 ml of 0.02 mol L^{-1} $MnCl_2$, $FeCl_3$, or $MnCl_2$ + $FeCl_3$ solution, the preparation scheme are shown in the Fig. S1, respectively, under magnetic stirring for 2 h. Then the solid samples were prepared under identical conditions to obtain BC-Mn, BC-Fe, and BC-Fe-Mn, respectively.

2.3 Simultaneous immobilization of lead, cadmium, and arsenic in soil: batch tests

The performance of the materials on the simultaneous immobilization of Pb, Cd, and As in soil were investigated through batch tests in 150 ml sealed plastic bottles, which contained 50 g of Pb, Cd, and As composite contaminated soil. Four different agents, i.e., BC, BC-Mn, BC-Fe, and BC-Fe-Mn were added to the soil system, respectively, with a dosage of 5 wt%. Water was added to the batch systems to maintain the water content at 80 wt%. Soil samples were withdrawn at different time points. Soil samples were naturally air-dried and crushed for further analyses. All experiments were performed at room temperature of 25 °C and carried out in triplicate.

2.4 Sample analysis

To investigate the effectiveness stabilization efficiency of heavy metals, the contents of $NaHCO_3$-extractable As and DTPA-extractable Pb and Cd in soil samples were assessed using the method described by Liang (YANG et al., 2018b) and McLaren (MCLAREN et al., 1998). The efficiency of the as-prepared materials in heavy metals immobilization (η) was calculated using Eq. 1:

$$\eta = \frac{C_0\text{-}C_t}{C_0} * 100\%$$

C_0 represents the initial leaching concentration of metals in soils; C_e refers to the leaching concentration of metals in soils after 90 days passivation.

The speciation distributions of Pb and Cd were assessed using a five-step sequential extraction method (SEP) (TESSIER et al., 1979); while, the speciation of arsenic was extracted according to the method of (WENZEL et al., 2001). These methods classify Pb and Cd in soil into five fractions namely; exchangeable fraction, carbonate bound fraction, Fe-Mn oxide bound fraction, organic bound fraction, and residual fraction, and classify As into five fractions: non-specific bound arsenic, specific bound arsenic, amorphous or low crystallinity iron bound arsenic, crystalline iron or aluminum oxide bound arsenic and arsenic residue.

2.5 Separation of magnetic particles in soil

10 g of the soil after immobilization was added into a 500 ml beaker, which contained 200 ml of deionized water. Then the suspension was placed on magnetic stirring apparatus at the stirring speed of 200 rpm for 2 h. After sealed in a self-sealing bag, the strong magnet was placed along the outside wall of the beaker to collect the magnetic materials. The collected materials were washed with deionized water for several times and dried at 40 °C.

2.6 Method of analysis

Soil pH was measured at a solid-water ratio of 1:2.5 using a pH meter. The BC and modified BC were characterized by scanning electron microscope (SEM, JSM-IT300LA, Japan), which was equipped with an energy dispersive spectrometer (EDS. JED-2300, Japan). X-ray photoelectron spectroscopy (XPS, Thermo Scientific K-Alpha, United States) was employed to characterize the element composition and valence states of the materials before and after reaction. The composition and crystalline structure of the materials were analyzed via an X-ray diffractometer (XRD, Rigaku D/max-2500, Japan). Fourier-transformed infrared (FTIR, Perkin Elmer, United States) were employed to detect the functional groups on the surface of the biochar.

3 Results and discussion

3.1 Fe and Mn modification of BC

Figure 1(a~d) displays the SEM and SEM-EDS images with element mapping of the modified BC. The BC had a tough structure with a rough and compact surface. In contrast, the modified BC possessed a porous structure. In order to explore the iron and manganese modification on the surface of BC, the SEM-coupled

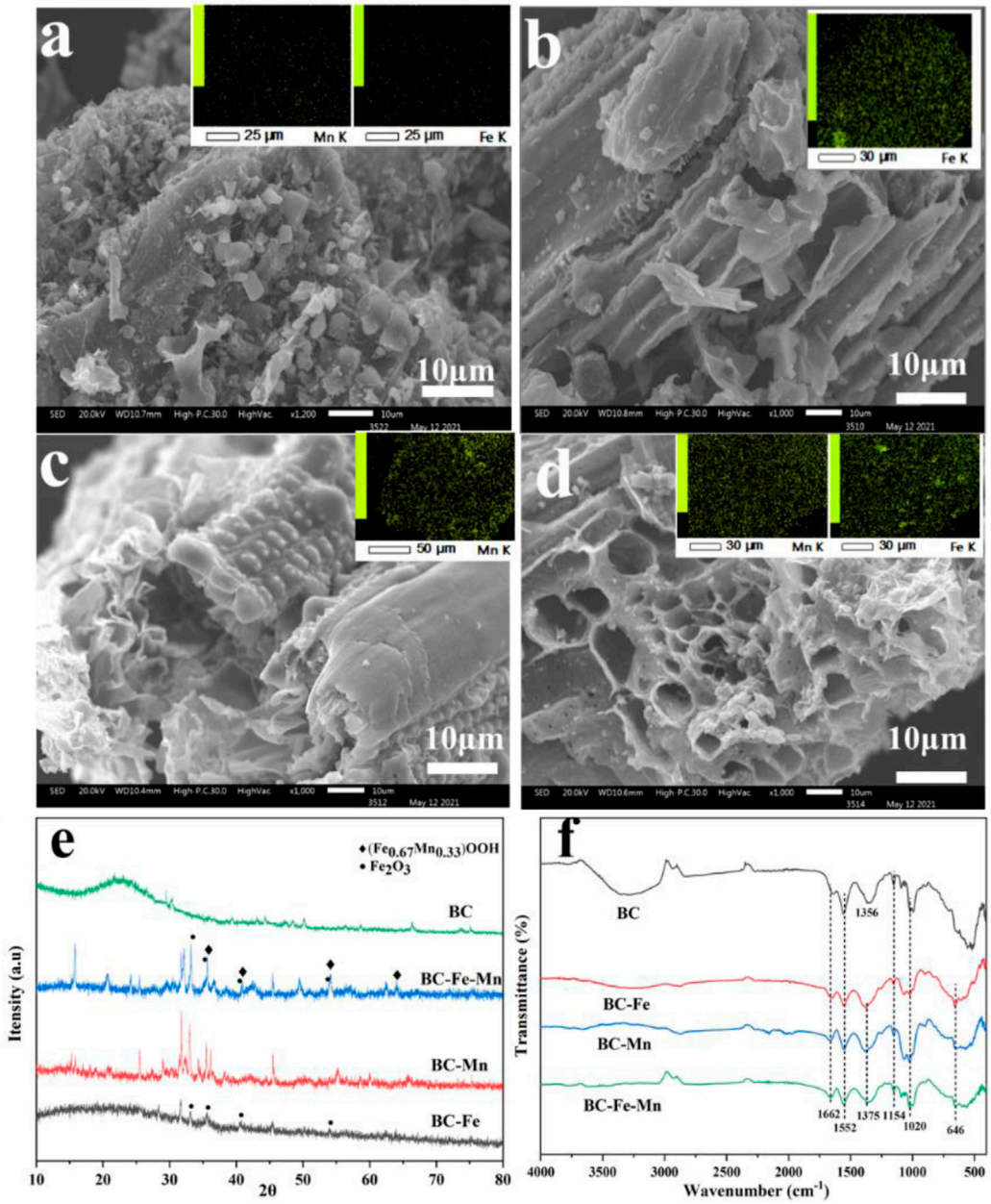

FIGURE 1
(A–D) SEM-EDS of BC **(A)**, BC-Fe **(B)**, BC-Mn **(C)**, and BC-Fe-Mn **(D)**; XRD **(E)** and FTIR **(F)** of different materials.

elemental mapping images of modified BC was analyzed. As shown in Figure 1A, almost no Fe and Mn existed on the surface of BC. However, after modification, Fe and Mn were evenly distributed on the surface of the materials. The properties of the BC-based materials prepared under various modified conditions are shown in Table 2. The content of C, H, O, and N atoms in BC decreased significantly. The C content of iron or/and manganese modified BC decreased by 12.7%–19.2% along with the introduction of metal elements. The C elements of BC participates in the reduction of metal elements and is consumed at high temperature during modification process (HOCH et al., 2008). Moreover, reduction of hydrogen and oxygen content generally involves dehydration and decarboxylation. As reported by Glaser et al., a BC with a low H/C ratio (<60%) and a low O/C ratio (<40%) has good stability and can be used as a soil conditioner (SCHIMMELPFENNIG and GLASER, 2012). Hence, the modified BC prepared in this study has the potential to improve the remediation.

The XRD pattern of the modified BC is shown in Figure 1E. There were no sharp absorption peaks of manganese after Mn modification. It indicated that manganese oxide might exist on BC in the form of amorphous phase. Conversely, after Fe modification, the diffraction peaks at 33.12°, 35.60°, 40.82°, and 54.00° in XRD patterns were associated with Fe_2O_3 (PDF#89–0,597). During high temperature calcination, $FeCl_3$ was converted into FeOOH and loaded on the BC as Fe_2O_3. When the $MnCl_2$ was introduced into the calcination, certian Mn might

TABLE 2 The basic properties of BC derived from the different modified conditions.

Sample	Elemental analysis					
	C (wt%)	H (wt%)	O (wt%)	N (wt%)	H/c (%)	O/C (%)
BC	54.24	2.43	13.36	1.27	4.48	24.63
BC-Fe	41.5	1.69	13.32	1.11	4.07	32.10
BC-Mn	35.49	1.99	13.95	0.96	5.61	39.31
BC-Fe-Mn	35.03	1.63	9.17	0.96	4.65	26.18

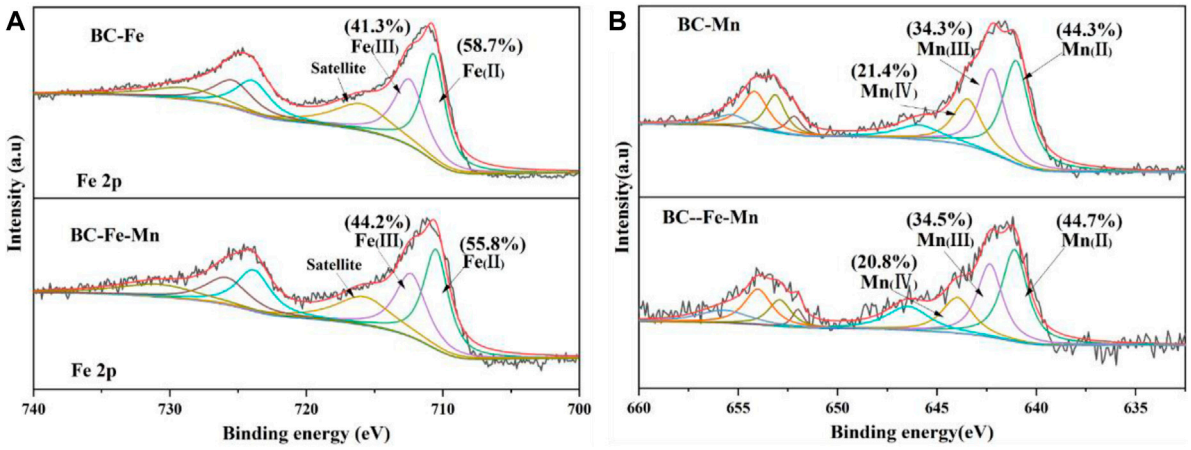

FIGURE 2
XPS spectra of the different types of BC. Fe2p XPS spectra of BC-Fe and BC-Fe-Mn **(A)**; Mn2p XPS spectra of BC-Mn and BC-Fe-Mn **(B)**.

replace Fe in FeOOH to form $(Fe_{0.67}Mn_{0.33})OOH$ during the transformation of FeOOH to Fe_2O_3 with the increase of calcination temperature (LI et al., 2022a). Accordingly, the application of Fe and Mn modification resulted in the appearance of two obvious peaks. The diffraction peaks at 35.67°, 40.99°, 54.23°, and 64.18° corresponded to $(Fe_{0.67}Mn_{0.33})OOH$ diffraction (PDF-#14–0,557), and the peaks at 33.12°, 35.60°, 40.82°, and 54.00° corresponded to the diffraction of Fe_2O_3 (PDF-#89–0,597). As shown in Figure 1F, FTIR was used to analyze the properties of the functional groups in BC. The absorption peak at 1,552 cm^{-1} corresponds to the stretching vibration of C-N, while peak at 1,662 cm^{-1} corresponds to the C-O vibration (LI et al., 2022b). The absorption peak at 1,356 cm^{-1} is attributed to the -COO vibration on the BC. It significantly shifts to 1,375 cm^{-1} in the modified BC, which might indicate that the introduction of iron or/and manganese during the modification (ZHANG et al., 2019a; TAN et al., 2022). The absorption peak at 646 cm^{-1} belongs to the absorption peak of Fe-O, which comes from the Fe-O vibration in Fe_2O_3 (LI et al., 2022a). These functional group structures suggest that the addition of iron results in the formation of new functional groups, whereas, the modified BC still retains its organic structures.

XPS analysis of the modified materials was carried out as Figure 2. Fe 2p and Mn 2p peaks were detected on the surface of BC after modification. The Fe 2p XPS spectra (Figure 2A) showed that the peaks at 712.5 eV and 710.8 eV were attributed to Fe(III) compounds and Fe(II) compounds, respectively (ZHU et al., 2020). While the peaks at 643.5, 641.8, and 640.8 eV (Figure 2B) were attributed to Mn(IV), Mn(III), and Mn(II) (TAN et al., 2022). On the surface of BC-Fe, Fe(III) accounted for 41.3% of the total surface atomic number of Fe. While on the surface of BC-Fe-Mn, the content of Fe(III) increased to 44.2%. At the same time, the proportion of Mn(IV) (20.8%) on the surface of BC-Fe-Mn was lower than that of BC-Mn (21.4%). It might be that certain Fe(II) was oxidized by the Mn(IV) to form Fe(III) as the introduction of iron and manganese during the calcination.

3.2 Simultaneous immobilization of Pb-Cd-As contaminated soil

Figure 3 shows the immobilization efficiency of Pb, Cd, and As by the BC as a function of time. After 90 days of remediation, only 6.5% and 20% of Pb and Cd were immobilized by BC, respectively. It proved that a great deal of Pb and Cd in soil could not be adsorbed onto BC. Moreover, the content of As in soil increased with the remediation. One of the possible reasons was that the addition of BC increased the pH value of the soil from 6.55 to 7.23, increasing the negative charge sites for the adsorption of metal cation. In contract, the competitive adsorption of BC with anionic arsenate resulted in the increase of available As in soil. Despite Fe modification, the

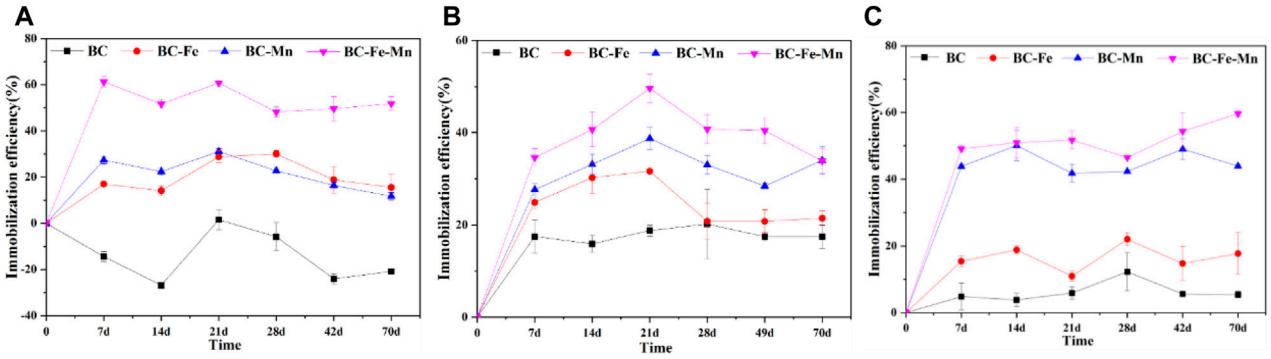

FIGURE 3
The immobilization efficiency of the various modified BC for As **(A)**, Cd **(B)**, and Pb **(C)** in soil with 5% addition of material as a function of time and material.

immobilization efficiency of As, Cd, and Pb remained low (15.5%, 21.5%, and 17.7%, respectively). The similar results were also observed by Wang et al. (WANG et al., 2020). As for the BC-Mn, the immobilization efficiency of As, Cd, and Pb increased at the initial stage (21 days) and then leveled out. The maximum immobilization efficiency of As, Cd, and Pb reached 31.1%, 38.8%, and 50.1%, respectively. During the BC-Fe-Mn remediation, the immobilization efficiencies increased with the reaction time. After 90 days, the immobilization efficiencies on Pb, Cd, and As reached 57%, 51% and 35%, respectively. Moreover, the water-soluble Pb and As were almost removed within 14 days, and more than 99% of the water-soluble Cd could be stabilized after 49 days (Fig. S2). The materials can be ranked based on their efficiency in the following order: BC-Fe-Mn > BC-Mn > BC-Fe > BC (Pb and Cd) and BC-Fe-Mn > BC-Fe > BC-Mn > BC (As). Therefore, BC-Fe-Mn exhibited the best immobilization efficiency for lead, cadmium and arsenic in soil.

3.3 Changes of soil properties

The pH of soil plays an important role in immobilization of heavy metals in soil. The application of BC resulted in a significant increase in the pH of soil (from 6.55 to 7.23, Table 3). During the pyrolysis process of the biomass, the base cations (primarily K, Ca, Na, Mg) were converted into oxides, hydroxides, and carbonates (HOUBEN et al., 2013). These alkaline substances dissolve and compete with As for the adsorption sites, resulting in As activation in soil. When the modified BC were employed in the soil remediation, the leaching of iron or manganese would cause the acidification of soil (TAO et al., 2019). Herein, the soil pH exhibited varying degrees of decrease after the application of modified BC (ranging from 6.55 to 5.66). Cd and Pb would be activated and released due to the acidification (MICHáLEKOVá-RICHV et al., 2016). The decreased pH also caused a decrease of negative charge in variable charge soil, thereby decreasing adsorption of cationic metals. Therefore, the slight change in the BC-Fe-Mn system will benefit the simultaneous immobilization of Pb, Cd, and As. The cation exchange capacity (CEC) is a dynamic component that affects the

TABLE 3 The basic properties of soil after the reaction was completed.

Material	CK	BC	BC-Fe	BC-Mn	BC-Fe-Mn
pH	6.55	7.23	5.66	5.71	6.07
CEC (cmol/kg $^{-1}$)	5.28	5.87	3.59	4.12	3.37

stability of soil. Upon completion of the reaction, CEC in soil changed significantly. In acidic soils, the disproportionate replacement of cations by H^+ results in a decrease in negative charge, which leads to a reduction in CEC (SHARMA et al., 2015). Thus, the reduction of CEC in soil may be the result of immobilization of the heavy metals during remediation (SONG et al., 2017).

3.4 Speciation distributions of Pb, Cd, and As

The relationship between the morphological transitions of BC-Fe-Mn and the immobilization efficiency of heavy metals in soil was studied. As shown in Figure 4, there was no non-specifically fraction of As in soil. With the extension of time, the content of specifically-sorbed As decreased by 10%. The amorphous iron bound As increased 9%. This may be due to the formation of stable iron arsenate compounds between As and Fe (SHAN and TONG, 2013). As for the Cd, the carbonate bound (CB) fraction showed a significant decrease from 19% to 8%. The content of Fe-Mn oxide bound (OM) fraction and residual fraction (RS) increased by 4% and 7%, respectively. Therefore, the environmentally sensitive fraction of Cd transformed into a more stable state. Meanwhile, the CB fraction of Pb decreased, and the RS and OM fraction increased. Pb generally exchanges with the Mg^{2+} and Ca^{2+} on the surface of BC to form stable complexes (LI et al., 2018; BANDARA et al., 2019). It interacts with–COO–, –O–and C–π on BC to generate organically bound fraction (SUN et al., 2021; T et al., 2015). Based on speciation analysis, it can be seen that Pb, Cd, and As can be converted to a more stable state under the effect of BC-Fe-Mn. And the amorphous iron bound (or OX fraction) and RS fraction are the main forms of Cd and As conversion, while OM fraction and RS fraction are the main forms of lead conversion.

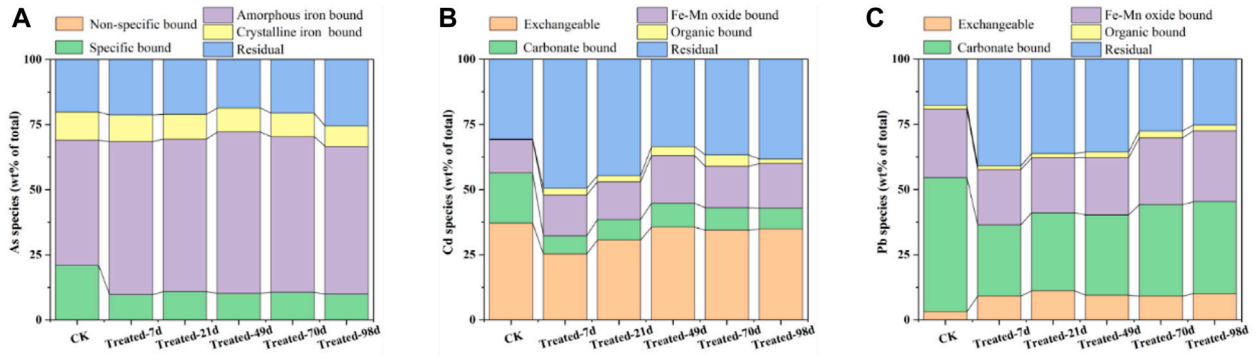

FIGURE 4
The SEP morphological changes of arsenic **(A)**, cadmium **(B)** and lead **(C)** in soil after BC-Fe-Mn modification.

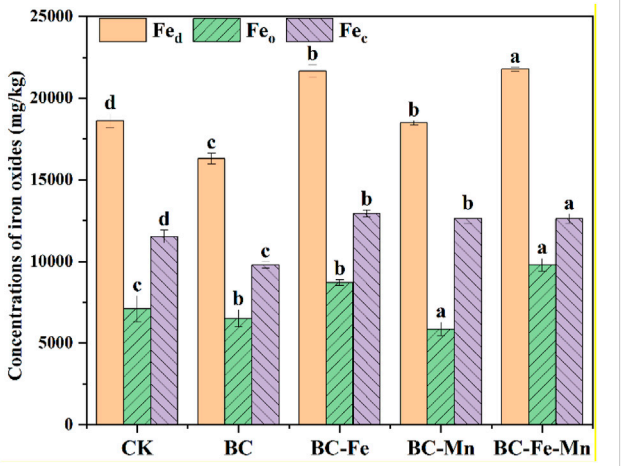

FIGURE 5
Soil iron oxide fractions after reaction. Fe_d, free iron oxides; Fe_o, amorphous iron oxides; and Fe_c, crystal iron oxides. Means (n = 3) followed by different letters above the columns indicate significant difference at $P < 0.05$.

3.5 Changes in iron oxide fractions

In soil, iron oxide is the main carrier of positive and negative charge and has a high affinity for heavy metals such as As, Cd, and Pb (GUO et al., 2021). Compared to CK, BC reduced the content of Fe_d, Fe_o, and Fe_c (Figure 5), indicating that the activity of iron oxide in soil was inhibited after BC application. This may be a potential explanation for the ineffective As immobilization following BC application. The content of Fe_d remained unchanged after the BC-Mn application, whereas the amount of Fe_o decreased and the amount of Fe_c increased. It suggested that additional manganese can promote transformation of iron into crystalline phase (LUO et al., 2018), leading to the aging of iron oxide in soil. When BC-Fe and BC-Fe-Mn were introduced into soil, it could be supplied as a iron source to convert into the unstable and poorly crystalline iron oxide (ferrihydrite) in soil via the hydrolysis of Fe^{2+} and Fe^{3+} (CUDENNEC and LECERF, 2006). Consequently, the Fe_d content increased from 18,622 mg kg^{-1} to 21,700 and 22,100 mg kg^{-1}, and the activity of iron in soil was enhanced. Compared with CK, the content of Fe_o in BC-Fe and BC-Fe-Mn system showed a substantial increase. It increased by 1700 mg kg^{-1} and 2,700 mg kg^{-1} after BC-Fe and BC-Fe-Mn application, respectively. It proved that manganese may enhance iron activation, when iron and manganese were coexist on BC (GASPARATO and S, 2012; ZHENG et al., 2020). As well known, Fe_d and Fe_o are effective Fe oxide components that facilitate the adsorption of metals by soil aggregates. Herein, the increase of Fe_d and Fe_o after BC-Fe-Mn application could improve the simultaneous immobilization.

3.6 Simultaneous immobilization mechanism in soil

BC-Fe-Mn significantly influence the form of iron oxides in soil and promotes the transformation of heavy metals into iron-manganese fractions. In order to further explore the immobilization mechanism of Pb, Cd, and As, the iron-containing magnetic particles (MPs) in soil were isolated and analyzed through XRD, XPS and SEM. MPs separated from soil after BC reaction presented as agglomeration state (Supplementary Figure S3). The MP extracted from the natural soil exhibited a granular structure, while the MP extracted from BC-based materials treated soil had a scale-like surface. The XRD patterns (Supplementary Figure S4) showed the MPs were mainly consisted of iron-manganese composite carboxyl oxide ($Fe_{0.67}Mn_{0.33}$)OOH (PDF-#14–0,557) and Fe_2O_3 (PDF-#33–0,664). This ($Fe_{0.67}Mn_{0.33}$)OOH molecule possessed abundant oxygen vacancies and -OH, which exhibited a strong affinity towards heavy metals (LI et al., 2022a).

Surface element results were shown in the Supplementary Table S1. The concentration of As and Cd on the surface of MP were significantly higher than that of soil. It suggested that the MP is one of the reaction sites of simultaneous immobilization in soil. After the BC-Fe-Mn application, the content of As on MP increased by 90.4% as compared with the CK. It might be due to that the released Fe reacted with the adsorbed As to form the iron-arsenic precipitation during the immobilization (SHAN and TONG, 2013). The XPS spectra of MP were shown in Figure 7. The peaks at 712.5 eV was attributed to Fe(III) $2p_{3/2}$. The peak at

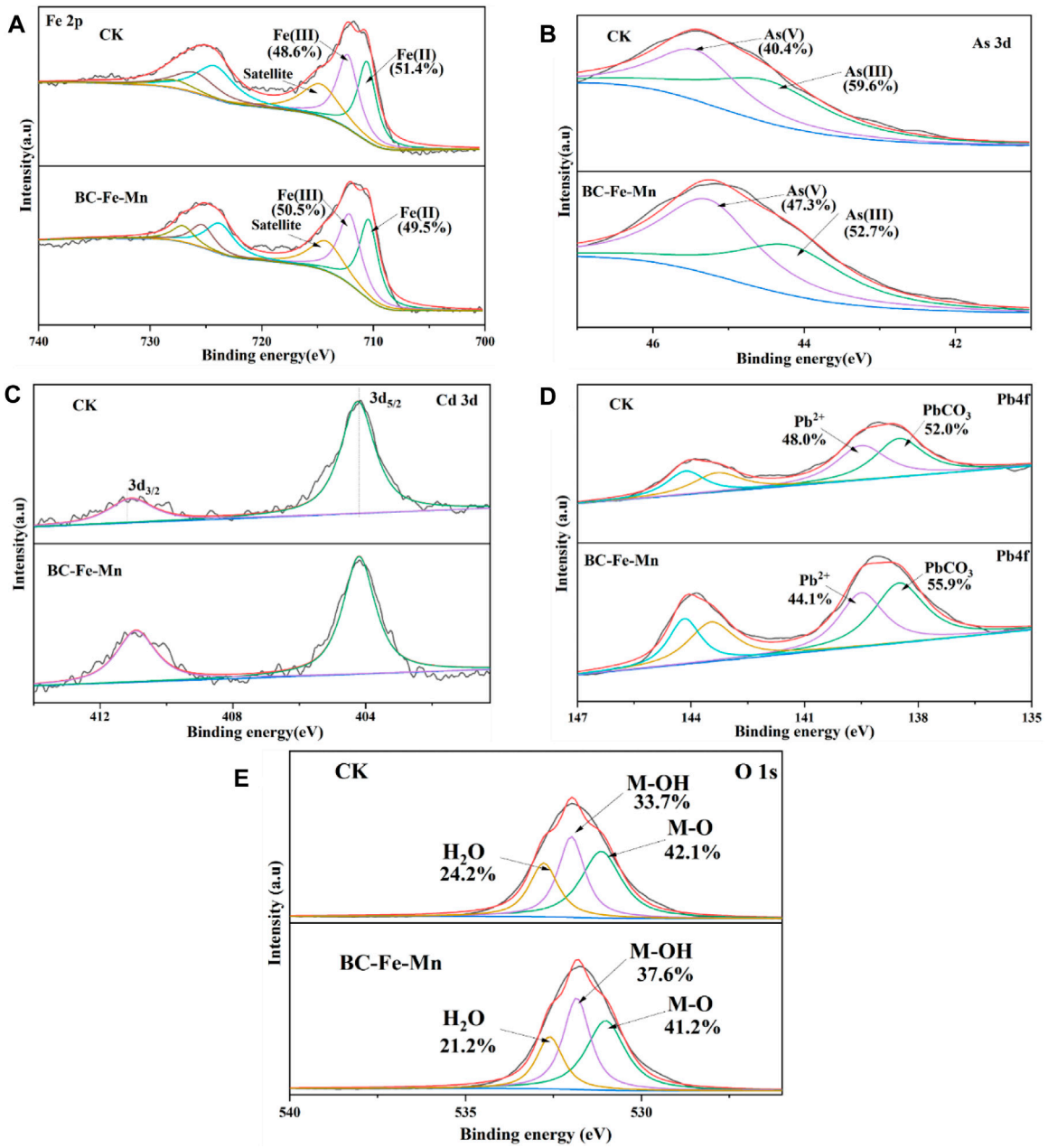

FIGURE 6
XPS spectrum of MP isolated from CK and BC-Fe-Mn treated soil. Fe 2p XPS spectra of CK and BC-Fe-Mn **(A)**; As 3d XPS spectra of CK and BC-Fe-Mn **(B)**; Cd 3d XPS spectra of CK and BC-Fe-Mn **(C)**; Pb 4f XPS spectra of CK and BC-Fe-Mn **(D)**; O 1s XPS spectra of CK and BC-Fe-Mn **(E)**.

710.2 eV was associated with the $2p_{3/2}$ orbitals from Fe(II) (ZHU et al., 2020). On the surface of MP separated from CK, the Fe species consisted of 51.4% Fe(II) and 48.6% Fe(III). While on the surface of MP isolated from BC-Fe-Mn reaction, the content of Fe(III) increased to 50.5%, and the content of Fe(II) decreased to 49.5%. This is probably due to the oxidative effect of Mn in BC-Fe-Mn, which could convert certain Fe(II) into Fe(III) (SUN et al., 2018). It is also possible that the iron oxide (iron hydride) generated by the hydrolysis of free ferric iron in the material adsorbed on the MP, increasing the content of Fe^{3+} (CUDENNEC and LECERF, 2006). Meanwhile, Figure 6B shown the peaks at 44.2 and 44.5 eV belonged to the signals of As(III) and As(V), respectively. The content of As(V) on the surface of MP from BC-Fe-Mn (47.3%) is higher than that from CK (40.4%), revealing the reduction of Mn(IV) → Mn(III) → Mn(II) might lead to effective As(III) oxidation to As(V).

Thus, the BC-Fe-Mn promoted the oxidation of As(III) during the remediation. The peaks at 411.6 eV and 404.8 eV were assigned to the $3d_{3/2}$ and $3d_{5/2}$ orbitals from Cd (Figure 6C), respectively (LIANG et al., 2017). It indicated that Cd was immobilized in the form of $Cd(OH)_2$ and Cd-Fe hydroxide (WANG et al., 2021a). Moreover, the peaks at 138.8 eV and 139.9 eV represented $PbCO_3$/PbO and Pb^{2+}, respectively (ZHANG et al., 2019b). The increased content of $PbCO_3$ (from 52.0% to 55.9%) showed that BC-Fe-Mn

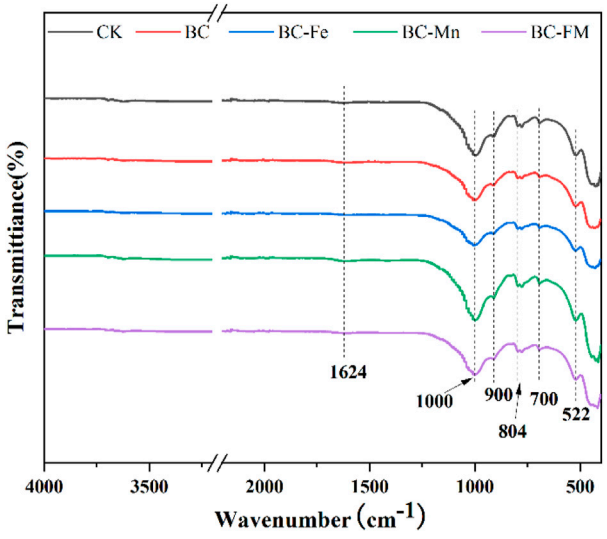

FIGURE 7
FTIR spectra of MP samples of BC-Fe-Mn, BC-Mn, BC-Fe, BC, and CK for 90 d.

induced the Pb immobilization in soil. The fitted O 1s spectrum (Figure 6E) presented three peaks at 530.8, 532.1 and 533.2 eV, characteristic of lattice oxygen (O^{2-}), hydroxyl (-OH), and adsorbed water (H_2O), respectively. Following remediation under BC-Fe-Mn, a reduction in O^{2-} moiety was observed from 42.1% to 41.2%. It suggested that the heavy metals gradually replaced the hydroxyl groups during sorption.

The FTIR spectra of the MPs are shown in Figure 7. The absorption peak at 522 cm^{-1} corresponds to the Mn-O vibration of MnO_6 octahedron (HOU et al., 2017), and the absorption peak near 1,624 cm^{-1} is the band of the O-H bending vibration band. The absorption peak around 890 cm^{-1} is associated with Fe-OH. The band at 900 cm^{-1} is assigned to -OH in goethite (XIAO et al., 2017). The peaks observed at 1,000 cm^{-1} and 700 cm^{-1} belongs to the Fe-OH and Mn-OH (XIAO et al., 2020) deformation vibration of iron-manganese oxides (XIONG et al., 2017; TAN et al., 2022). In general, the vacancies of manganese and iron oxides lead to the double-coordinated unsaturation, which tend to form O- and adsorb protons to form stable -OH to achieve charge balance. Thus, Mn-O and Fe-O can bond with heavy metals. Heavy metal cations in soils compete with protons to occupy the adsorption sites on iron-manganese oxides due to their strong charge interaction (LIN et al., 2020; JIN et al., 2022). Therefore, Mn-O and Fe-O are important functional groups for Cd immobilization. After immobilization, the peaks of Fe/Mn-OH appeared at higher wavenumbers, which may be attributed the decrease in the bond strength of Fe/Mn-O due to the solid electron donating effect of Cd in Fe/Mn-O-Cd (PENG et al., 2015; WANG et al., 2021b). The absorption peak at 816 cm^{-1} corresponded to As-OH or As-O-Fe stretching vibration. (HAN et al., 2016). Probably indicating the participation of As on MPs through the formation of an internal spherical bidentate binuclear complex adsorption (LIN et al., 2020). Furthermore, the formation of Fe-O-As(V) complex is also responsible for the adsorption of As(V) to Fe-O due to the strong binding ability of arsenic and iron (SHAN and TONG, 2013). It further proved that As also adsorbed on the surface of iron and manganese oxides.

Fe_2O_3 and $(Fe_{0.67}Mn_{0.33})OOH$ played an important role in the immobilization of heavy metals in soil. When the BC-Fe-Mn was introduced, Cd and Pb were absorbed and combined with OH, C-π, -COO functional groups on BC-Fe-Mn. As(III) firstly adsorbed on the surface of BC-Fe-Mn. The more electro-positive standard redox potential of the Fe(III)/Fe(II) couple (+0.771 V), the Mn(III)/Mn(II) couple (+1.51 V), and the Mn(IV)/Mn(II) couple (+1.23 V) than that of As(V)/As(III) (+0.56 V) enables the oxidation of As(III) by Mn(IV) and Mn(III), as described by Eq. 1–Eq. 3:

$$2Fe^{3+} + HAsO_2 + 2H_2O \rightarrow Fe^{2+} + H_3AsO_4 + 4H^+ \quad (1)$$

$$2MnO_4^- + 5HAsO_2 + 6H^+ + 2H_2O \rightarrow 2Mn^{2+} + 5H_3AsO_4 \quad (2)$$

$$MnO_2 + HAsO_2 + 2H^+ \rightarrow Mn^{2+} + H_3AsO_4 \quad (3)$$

$$2Fe^{2+} + MnO_2 + 4H^+ \rightarrow 2Fe^{3+} + Mn^{2+} + 2H_2O \quad (4)$$

$$5Fe^{2+} + MnO_4^- + 8H^+ \rightarrow 5Fe^{3+} + Mn^{2+} + 4H_2O \quad (5)$$

Moreover, the standard redox potential of the MnO_2/Mn^{2+} and MnO_4^-/Mn^{2+} is also more electro-positive than that of Fe^{3+}/Fe^{2+}, thus Mn oxides are capable of oxidizing Fe^{2+} to Fe^{3+} as described by Eq. (4-5). Then, the reduction of Mn(IV) → Mn(III) → Mn(II) leads to effective As(III) oxidation to As(V). Meanwhile, Fe/Mn in BC-Fe-Mn hydrolyzed to generate protons, thereby reducing the pH of the soil. The decrease in pH activated iron oxides in soil, leading to an increase in free iron oxides. The free iron oxide then reacted with dissolved As, resulting in iron-arsenic precipitation and an increase in As immobilization in soil. After treatment with BC-Fe-Mn, As and Cd transformed to the Fe-Mn oxide bound fraction, while Pb transformed to the residual fraction in soil.

4 Conclusion

In this study, iron and manganese were employed to modified the BC. The obtained BC-Fe-Mn could reduce the content of available As, Cd, and Pb by 35%, 51%, and 57% in soil. It also promoted the heavy metals to transform from the available state into relative stable state. Moreover, simultaneous immobilization mechanisms have been detected. It might involve heavy metal morphological transformation, precipitation/co-precipitation, and surface complexation. During the procedure, Cd and Pb absorbed and combined with OH, C-π, -COO functional groups on BC-Fe-Mn. BC-Fe-Mn promoted the increase of free iron oxides, which reacted with the dissolved As to form iron-arsenic precipitation. This work provides a promising remediation strategy for simultaneous immobilization of Pb, Cd, and As in soil and promote the insight of simultaneous immobilization mechanisms.

Data availability statement

The original contributions presented in the study are included in the article/Supplementary Material, further inquiries can be directed to the corresponding author.

Author contributions

ZY: Project administration, Supervision, Writing–original draft. GZ: Formal Analysis, Investigation, Methodology, Visualization, Writing–original draft. LL: Methodology, Writing–review and editing. FH: Formal Analysis, Writing–review and editing. CA: Writing–review and editing. QL: Writing–review and editing. WY: Writing–review and editing. MS: Conceptualization, Investigation, Methodology, Writing–review and editing.

Funding

The author(s) declare financial support was received for the research, authorship, and/or publication of this article. This work was financially supported by National Natural Science Foundation of China (U20A20267) and Major Program Natural Science Foundation of Hunan Province of China (2021JC0001).

Conflict of interest

The authors declare that the research was conducted in the absence of any commercial or financial relationships that could be construed as a potential conflict of interest.

Publisher's note

All claims expressed in this article are solely those of the authors and do not necessarily represent those of their affiliated organizations, or those of the publisher, the editors and the reviewers. Any product that may be evaluated in this article, or claim that may be made by its manufacturer, is not guaranteed or endorsed by the publisher.

Supplementary material

The Supplementary Material for this article can be found online at: https://www.frontiersin.org/articles/10.3389/fenvs.2023.1281341/full#supplementary-material

References

Bakshi, S., Banik, C., Rathke, S. J., and Laird, D. A. (2018). Arsenic sorption on zero-valent iron-biochar complexes. *Water Res.* 137, 153–163. doi:10.1016/j.watres.2018.03.021

Bandara, T., Franks, A., Xu, J., Bolan, N., Wang, H., and Tang, C. (2019). Chemical and biological immobilization mechanisms of potentially toxic elements in biochar-amended soils. *Crit. Rev. Environ. Sci. Technol.* 50 (9), 903–978. doi:10.1080/10643389.2019.1642832

Chen, D., Liu, W., Wang, Y., and Lu, P. (2021). Effect of biochar aging on the adsorption and stabilization of Pb in soil. *J. Soils Sediments* 22 (1), 56–66. doi:10.1007/s11368-021-03059-x

Cudennec, Y., and Lecerf, A. (2006). The transformation of ferrihydrite into goethite or hematite, revisited. *J. solid state Chem.* 179 (3), 716–722. doi:10.1016/j.jssc.2005.11.030

Cui, H., Zhang, X., Wu, Q., Zhang, S., Xu, L., Zhou, J., et al. (2020). Hematite enhances the immobilization of copper, cadmium and phosphorus in soil amended with hydroxyapatite under flooded conditions. *Sci. Total Environ.* 708, 134590. doi:10.1016/j.scitotenv.2019.134590

Fu, D., He, Z., Su, S., Xu, B., Liu, Y., and Zhao, Y. (2017). Fabrication of α-FeOOH decorated graphene oxide-carbon nanotubes aerogel and its application in adsorption of arsenic species. *J. Colloid Interface Sci.* 505, 105–114. doi:10.1016/j.jcis.2017.05.091

Gao, Z., Fu, W., Zhang, M., Zhao, K., Tunney, H., and Guan, Y. (2016). Potentially hazardous metals contamination in soil-rice system and it's spatial variation in Shengzhou City, China. *J. Geochem. Explor.* 167, 62–69. doi:10.1016/j.gexplo.2016.05.006

Gasparatos, D. (2012). Sequestration of heavy metals from soil with Fe–Mn concretions and nodules. *Environ. Chem. Lett.* 11 (1), 1–9. doi:10.1007/s10311-012-0386-y

Guo, Y., Li, X., Liang, L., Lin, Z., Su, X., and Zhang, W. (2021). Immobilization of cadmium in contaminated soils using sulfidated nanoscale zero-valent iron: effectiveness and remediation mechanism. *J. Hazard. Mater.* 420, 126605. doi:10.1016/j.jhazmat.2021.126605

Han, X., Song, J., Li, Y.-L., Jia, S. Y., Wang, W. H., Huang, F. G., et al. (2016). As(III) removal and speciation of Fe (Oxyhydr)oxides during simultaneous oxidation of As(III) and Fe(II). *Chemosphere* 147, 337–344. doi:10.1016/j.chemosphere.2015.12.128

Hoch, L. B., Mack, E. J., Hydutsky, B. W., Hershman, J. M., Skluzacek, J. M., and Mallouk, T. E. (2008). Carbothermal synthesis of carbon-supported nanoscale zero-valent iron particles for the remediation of hexavalent chromium. *Environ. Sci. Technol.* 42 (7), 2600–2605. doi:10.1021/es702589u

Hou, J., Luo, J., Song, S., Li, Y., and Li, Q. (2017). The remarkable effect of the coexisting arsenite and arsenate species ratios on arsenic removal by manganese oxide. *Chem. Eng. J.* 315, 159–166. doi:10.1016/j.cej.2016.12.115

Houben, D., Evrard, L., and Sonnet, P. (2013). Mobility, bioavailability and pH-dependent leaching of cadmium, zinc and lead in a contaminated soil amended with biochar. *Chemosphere* 92 (11), 1450–1457. doi:10.1016/j.chemosphere.2013.03.055

Hu, Q., Liu, Y., Gu, X., and Zhao, Y. (2017). Adsorption behavior and mechanism of different arsenic species on mesoporous MnFe 2 O 4 magnetic nanoparticles. *Chemosphere* 181, 328–336. doi:10.1016/j.chemosphere.2017.04.049

Igalavithana, A. D., Kwon, E. E., Vithanage, M., Rinklebe, J., Moon, D. H., Meers, E., et al. (2019). Soil lead immobilization by biochars in short-term laboratory incubation studies. *Environ. Int.* 127, 190–198. doi:10.1016/j.envint.2019.03.031

Jin, C., Li, Z., Huang, M., Ding, X., Zhou, M., Cai, C., et al. (2022). Cadmium immobilization in lake sediment using different crystallographic manganese oxides: performance and mechanism. *J. Environ. Manag.* 313, 114995. doi:10.1016/j.jenvman.2022.114995

Kameda, K., Hashimoto, Y., Wang, S.-L., Hirai, Y., and Miyahara, H. (2017). Simultaneous and continuous stabilization of as and Pb in contaminated solution and soil by a ferrihydrite-gypsum sorbent. *J. Hazard. Mater.* 327, 171–179. doi:10.1016/j.jhazmat.2016.12.039

Li, B., Yang, L., Wang, C.-Q., Zhang, Q. p., Liu, Q. c., Li, Y. d., et al. (2017). Adsorption of Cd(II) from aqueous solutions by rape straw biochar derived from different modification processes. *Chemosphere* 175, 332–340. doi:10.1016/j.chemosphere.2017.02.061

Li, H., Li, Z., Khaliq, M. A., Xie, T., Chen, Y., and Wang, G. (2019). Chlorine weaken the immobilization of Cd in soil-rice systems by biochar. *Chemosphere* 235, 1172–1179. doi:10.1016/j.chemosphere.2019.06.203

Li, H., Xu, H., Zhou, S., Yu, Y., Zhou, Li, H. C., et al. (2018). Distribution and transformation of lead in rice plants grown in contaminated soil amended with biochar and lime. *Ecotoxicol. Environ. Saf.* 165, 589–596. doi:10.1016/j.ecoenv.2018.09.039

Li, M., He, Z., Zhong, H., Sun, W., Hu, L., and Luo, M. (2022a). Fe0.67Mn0.33)OOH riched in oxygen vacancies facilitated the PMS activation of modified EMR for refractory foaming agent removal from mineral processing wastewater. *Chem. Eng. J.* 441, 136024. doi:10.1016/j.cej.2022.136024

Li, Q., Liang, W., Liu, F., Wang, G., Wan, J., Zhang, W., et al. (2022b). Simultaneous immobilization of arsenic, lead and cadmium by magnesium-aluminum modified biochar in mining soil. *J. Environ. Manag.* 310, 114792. doi:10.1016/j.jenvman.2022.114792

Liang, J., Li, X., Yu, Z., Zeng, G., Luo, Y., Jiang, L., et al. (2017). Amorphous MnO2 modified biochar derived from aerobically composted swine manure for adsorption of Pb (II) and Cd (II). *ACS Sustain. Chem. Eng.* 5 (6), 5049–5058. doi:10.1021/acssuschemeng.7b00434

Lin, L., Li, J., Yang, X., Yan, X., Feng, T., Liu, Z., et al. (2020). Simultaneous immobilization of arsenic and cadmium in paddy soil by Fe-Mn binary oxide. *Elem. Sci. Anthropocene* 8 (1). doi:10.1525/elementa.2020.094

Luo, Y., Ding, J., Shen, Y., Tan, W., Qiu, G., and Liu, F. (2018). Symbiosis mechanism of iron and manganese oxides in oxic aqueous systems. *Chem. Geol.* 488, 162–170. doi:10.1016/j.chemgeo.2018.04.030

Lv, G., Yang, T., Chen, Y., Hou, H., Liu, X., Li, J., et al. (2021). Biochar-based fertilizer enhanced Cd immobilization and soil quality in soil-rice system. *Ecol. Eng.* 171, 106396. doi:10.1016/j.ecoleng.2021.106396

Lyu, H., Zhao, H., Tang, J., Gong, Y., Huang, Y., Wu, Q., et al. (2018). Immobilization of hexavalent chromium in contaminated soils using biochar supported nanoscale iron sulfide composite. *Chemosphere* 194, 360–369. doi:10.1016/j.chemosphere.2017.11.182

Mclaren, R. G., Naidu, R., Smith, J., and Tiller, K. G. (1998). *Fractionation and distribution of arsenic in soils contaminated by cattle dip*. Hoboken, New Jersey, U.S.A: Wiley Online Library.

MichálEKOVá-Richveisová, B., FrišťáK, V., PipíŠKA, M., Ďuriška, L., Moreno-Jimenez, E., and Soja, G. (2016). Iron-impregnated biochars as effective phosphate sorption materials. *Environ. Sci. Pollut. Res.* 24 (1), 463–475. doi:10.1007/s11356-016-7820-9

O'Reilly, S. E., and Hochella, M. F. (2003). Lead sorption efficiencies of natural and synthetic Mn and Fe-oxides. *Geochimica Cosmochimica Acta* 67 (23), 4471–4487. doi:10.1016/s0016-7037(03)00413-7

Peng, L., Zeng, Q., Tie, B., Lei, M., Yang, J., Luo, S., et al. (2015). Manganese Dioxide nanosheet suspension: a novel absorbent for Cadmium(II) contamination in waterbody. *J. Colloid Interface Sci.* 456, 108–115. doi:10.1016/j.jcis.2015.06.017

Ren, Y., Li, N., Feng, J., Luan, T., Wen, Q., Li, Z., et al. (2012). Adsorption of Pb(II) and Cu(II) from aqueous solution on magnetic porous ferrospinel MnFe2O4. *J. Colloid Interface Sci.* 367 (1), 415–421. doi:10.1016/j.jcis.2011.10.022

Schimmelpfennig, S., and Glaser, B. (2012). One step forward toward characterization: some important material properties to distinguish biochars. *J. Environ. Qual.* 41 (4), 1001–1013. doi:10.2134/jeq2011.0146

Shan, C., and Tong, M. (2013). Efficient removal of trace arsenite through oxidation and adsorption by magnetic nanoparticles modified with Fe–Mn binary oxide. *Water Res.* 47 (10), 3411–3421. doi:10.1016/j.watres.2013.03.035

Sharma, A., Weindorf, D. C., Wang, D., and Chakraborty, S. (2015). Characterizing soils via portable X-ray fluorescence spectrometer: 4. Cation exchange capacity (CEC). *Geoderma* 239-240, 130–134. doi:10.1016/j.geoderma.2014.10.001

Song, B., Zeng, G., Gong, J., Liang, J., Xu, P., Liu, Z., et al. (2017). Evaluation methods for assessing effectiveness of *in situ* remediation of soil and sediment contaminated with organic pollutants and heavy metals. *Environ. Int.* 105, 43–55. doi:10.1016/j.envint.2017.05.001

Song, Z., Lian, F., Yu, Z., Zhu, L., Xing, B., and Qiu, W. (2014). Synthesis and characterization of a novel MnOx-loaded biochar and its adsorption properties for Cu2+ in aqueous solution. *Chem. Eng. J.* 242, 36–42. doi:10.1016/j.cej.2013.12.061

Sun, Q., Cui, P.-X., Fan, T.-T., Wu, S., Zhu, M., Alves, M. E., et al. (2018). Effects of Fe(II) on Cd(II) immobilization by Mn(III)-rich δ-MnO2. *Chem. Eng. J.* 353, 167–175. doi:10.1016/j.cej.2018.07.120

Sun, T., Xu, Y., Sun, Y., Wang, L., Liang, X., and Jia, H. (2021). Crayfish shell biochar for the mitigation of Pb contaminated water and soil: characteristics, mechanisms, and applications. *Environ. Pollut.* 271, 116308. doi:10.1016/j.envpol.2020.116308

Tan, X., Liu, Y., Zeng, G., Wang, X., Hu, X., Gu, Y., et al. (2015). Application of biochar for the removal of pollutants from aqueous solutions. *Chemosphere* 125, 70–85. doi:10.1016/j.chemosphere.2014.12.058

Tack, F. M. G., Van Ranst, E., Lievens, C., and Vandenberghe, R. (2006). Soil solution Cd, Cu and Zn concentrations as affected by short-time drying or wetting: the role of hydrous oxides of Fe and Mn. *Geoderma* 137 (1-2), 83–89. doi:10.1016/j.geoderma.2006.07.003

Tan, W.-T., Zhou, H., Tang, S.-F., Zeng, P., Gu, J. F., and Liao, B. H. (2022). Enhancing Cd(II) adsorption on rice straw biochar by modification of iron and manganese oxides. *Environ. Pollut.* 300, 118899. doi:10.1016/j.envpol.2022.118899

Tao, H.-Y., Ge, H., Shi, J., Liu, X., Guo, W., Zhang, M., et al. (2019). The characteristics of oestrone mobility in water and soil by the addition of Ca-biochar and Fe–Mn-biochar derived from Litchi chinensis Sonn. *Environ. Geochem. Health* 42 (6), 1601–1615. doi:10.1007/s10653-019-00477-2

Tessier, A., Campbell, P. G., and Bisson, M. (1979). Sequential extraction procedure for the speciation of particulate trace metals. *Anal. Chem.* 51 (7), 844–851. doi:10.1021/ac50043a017

TóTH, G., Hermann, T., Da Silva, M. R., and Montanarella, L. (2016). Heavy metals in agricultural soils of the European Union with implications for food safety. *Environ. Int.* 88, 299–309. doi:10.1016/j.envint.2015.12.017

Tu, C., Wei, J., Guan, F., Liu, Y., Sun, Y., and Luo, Y. (2020). Biochar and bacteria inoculated biochar enhanced Cd and Cu immobilization and enzymatic activity in a polluted soil. *Environ. Int.* 137, 105576. doi:10.1016/j.envint.2020.105576

Villalobos, M., Escobar-Quiroz, I. N., and Salazar-Camacho, C. (2014). The influence of particle size and structure on the sorption and oxidation behavior of birnessite: I. Adsorption of As(V) and oxidation of As(III). *Geochimica Cosmochimica Acta* 125, 564–581. doi:10.1016/j.gca.2013.10.029

Wang, M., Hu, C., Xu, J., Jing, X., Rahim, H. U., and Cai, X. (2021a). Facile combinations of thiosulfate and zerovalent iron synergically immobilize cadmium in soils through mild extraction and facilitated immobilization. *J. Hazard. Mater.* 407, 124806. doi:10.1016/j.jhazmat.2020.124806

Wang, W., Lu, T., Liu, L., Yang, X., Sun, X., Qiu, G., et al. (2021b). Zeolite-supported manganese oxides decrease the Cd uptake of wheat plants in Cd-contaminated weakly alkaline arable soils. *J. Hazard. Mater.* 419, 126464. doi:10.1016/j.jhazmat.2021.126464

Wang, Y.-M., Wang, S.-W., Wang, C.-Q., Zhang, Z. y., Zhang, J. q., Meng, M., et al. (2020). Simultaneous immobilization of soil Cd(II) and as(V) by Fe-modified biochar. *Int. J. Environ. Res. Public Health* 17 (3), 827. doi:10.3390/ijerph17030827

Wenzel, W. W., Kirchbaumer, N., Prohaska, T., Stingeder, G., Lombi, E., and Adriano, D. C. (2001). Arsenic fractionation in soils using an improved sequential extraction procedure. *Anal. Chim. acta* 436 (2), 309–323. doi:10.1016/s0003-2670(01)00924-2

Xiao, J., Hu, R., Chen, G., and Xing, B. (2020). Facile synthesis of multifunctional bone biochar composites decorated with Fe/Mn oxide micro-nanoparticles: physicochemical properties, heavy metals sorption behavior and mechanism. *J. Hazard. Mater.* 399, 123067. doi:10.1016/j.jhazmat.2020.123067

Xiao, W., Jones, A. M., Collins, R. N., Bligh, M. W., and Waite, T. D. (2017). Use of fourier transform infrared spectroscopy to examine the Fe(II)-Catalyzed transformation of ferrihydrite. *Talanta* 175, 30–37. doi:10.1016/j.talanta.2017.07.018

Xiong, Y., Tong, Q., Shan, W., Xing, Z., Wang, Y., Wen, S., et al. (2017). Arsenic transformation and adsorption by iron hydroxide/manganese dioxide doped straw activated carbon. *Appl. Surf. Sci.* 416, 618–627. doi:10.1016/j.apsusc.2017.04.145

Yang, X., Igalavithana, A. D., Oh, S.-E., Nam, H., Zhang, M., Wang, C. H., et al. (2018a). Characterization of bioenergy biochar and its utilization for metal/metalloid immobilization in contaminated soil. *Sci. Total Environ.* 640-641, 704–713. doi:10.1016/j.scitotenv.2018.05.298

Yang, Z., Liang, L., Yang, W., Shi, W., Tong, Y., Chai, L., et al. (2018b). Simultaneous immobilization of cadmium and lead in contaminated soils by hybrid bio-nanocomposites of fungal hyphae and nano-hydroxyapatites. *Environ. Sci. Pollut. Res.* 25 (12), 11970–11980. doi:10.1007/s11356-018-1492-6

Zhang, J., Shao, J., Jin, Q., Li, Z., Zhang, X., Chen, Y., et al. (2019b). Sludge-based biochar activation to enhance Pb(II) adsorption. *Fuel* 252, 101–108. doi:10.1016/j.fuel.2019.04.096

Zhang, L., Guo, J., Huang, X., Wang, W., Sun, P., Li, Y., et al. (2019a). Functionalized biochar-supported magnetic MnFe2O4 nanocomposite for the removal of Pb(ii) and Cd(ii). *RSC Adv.* 9 (1), 365–376. doi:10.1039/c8ra09061k

Zheng, Q., Hou, J., Hartley, W., Ren, L., Wang, M., Tu, S., et al. (2020). As(III) adsorption on Fe-Mn binary oxides: are Fe and Mn oxides synergistic or antagonistic for arsenic removal? *Chem. Eng. J.* 389, 124470. doi:10.1016/j.cej.2020.124470

Zhou, Q., Lin, L., Qiu, W., Song, Z., and Liao, B. (2018). Supplementation with ferromanganese oxide–impregnated biochar composite reduces cadmium uptake by indica rice (Oryza sativa L.). *J. Clean. Prod.* 184, 1052–1059. doi:10.1016/j.jclepro.2018.02.248

Zhu, S., Qu, T., Irshad, M. K., and Shang, J. (2020). Simultaneous removal of Cd(II) and As(III) from co-contaminated aqueous solution by α-FeOOH modified biochar. *Biochar* 2 (1), 81–92. doi:10.1007/s42773-020-00040-8